https://doi.org/10.5194/acp-2021-1099
Preprint. Discussion started: 26 April 2022

Atmospheric Chemistry and Physics Discussions

Diagnosing the stratospheric proportion in tropospheric ozone using triple oxygen isotopes as tracers

Hao Xu[1], Urumu Tsunogai[1], Fumiko Nakagawa[1], Keiichi Sato[2], and Hiroshi Tanimoto[3]

[1]Graduate School of Environmental Studies, Nagoya University, Furo-cho, Chikusa-ku, Nagoya 464-8601, Japan
[2]Asia Center for Air Pollution Research, 1182 Sowa, Nishi-ku, Niigata-shi, 950-2144, Japan
[3] National Institute for Environmental Studies, 16-2 Onogawa, Tsukuba, Ibaraki 305-8506, Japan

Correspondence to: Hao Xu (xuhao1990kyokou@hotmail.co.jp)

Abstract. Using a multistep nitrite-coated filter-pack system for sampling, we determined the seasonal variations in the triple oxygen isotopic composition ($\Delta^{17}O$) of tropospheric ozone (O_3) in the terminal positions ($\Delta^{17}O_{term}(O_3)$) in the cities Nagoya and Niigata (Japan) in the eastern Asia region to quantify the mixing ratio of stratospheric O_3 within the total tropospheric O_3 supplied by stratosphere–troposphere transport (STT). In Nagoya, diurnal variations have also been studied. Both the average $\Delta^{17}O_{term}(O_3)$ and their 1σ variation ranges agreed well with previous studies, (37.5 ± 1.4) ‰ in Nagoya and (37.0 ± 1.7) ‰ in Niigata. The average difference in $\Delta^{17}O_{term}(O_3)$ between daytime (higher) and nighttime (lower) was (1.4 ± 0.7) ‰ (1σ) in Nagoya, which was responsible for the formation of a stable boundary layer at night, reducing mixing with high $\Delta^{17}O_{term}(O_3)$ from the free troposphere. We also found a significant correlation between ^7Be activity concentrations and the $\Delta^{17}O_{term}(O_3)$, implying that STT was responsible for the elevated $\Delta^{17}O_{term}$ of O_3 in the troposphere. By using the relationship between the reciprocal of concentrations and $\Delta^{17}O_{term}$ of tropospheric O_3, we estimated the $\Delta^{17}O$ of stratospheric O_3 supplied through the STT ($\Delta^{17}O_{STT}$), together with that produced through photochemical reactions at surface altitude ($\Delta^{17}O_{sur}$). Moreover, using $\Delta^{17}O_{STT}$ and $\Delta^{17}O_{sur}$, we estimated the mixing ratios of stratospheric O_3 (i.e., O_3 produced in the stratosphere and supplied to the troposphere through STT) in each tropospheric O_3 (f_{STT}), as well as the absolute concentrations of stratospheric O_3 supplied through STT in the troposphere ($C_{STT}(O_3)$). The $C_{STT}(O_3)$ exhibited minimum values in summer ((5.3 ± 1.0) ppb) and maximum values in late winter to spring ((15.9 ± 2.1) ppb). Although the f_{STT} values were higher than those estimated using the chemistry climate models from past studies, the trends of the seasonal variations were consistent with them. We concluded that $\Delta^{17}O$ successfully provided observational constraints on the STT of O_3.

1 Introduction

1.1 Tropospheric ozone and stratosphere–troposphere transport

Tropospheric ozone (O_3) plays an important role in environmental problems, including global climate change (Akimoto, 2003; Hansen and Sato, 2001; UNEP and WMO, 2011). Excess levels of tropospheric O_3 can significantly damage forests (Skärby et al., 1998), crops (Avnery et al., 2011; Reich and Amundson, 1985), and human health (Jerrett et al., 2009; Silva et al., 2013; Zhang et al., 2019). Additionally, O_3 and its reaction products, such as hydroxyl radicals (OH), control the oxidizing capacity of the troposphere and the oxidation rates and pathways of trace gases (Finlayson-Pitts and Pitts, 1997; Thompson, 1992), such as nitrogen oxides (NO_x = nitric oxide (NO) + nitrogen dioxide (NO_2)).

The concentration of O_3 in the troposphere is controlled by complex processes, such as in situ production through photochemical reactions of trace components (such as NO_2), dry deposition onto ground/ocean surfaces, lateral transport in the troposphere, and vertical transport from the stratosphere (Logan, 1985; Wild, 2007). Because the stratosphere is a large reservoir of O_3, stratosphere-troposphere transport (STT) is an important factor controlling the levels of tropospheric O_3. However, STT events are sporadic and not well characterized (Stohl et al., 2003b, 2003a). In addition, global warming will cause STT to increase in the future (Sudo et

https://doi.org/10.5194/acp-2021-1099
Preprint. Discussion started: 26 April 2022

Atmospheric Chemistry and Physics Discussions

al., 2003). Therefore, to better understand the factors controlling the levels of tropospheric O_3, we must quantify O_3 supplied through STT.

Traditionally, the radionuclide Beryllium-7 (^{7}Be; half-life of 53.3 days) has been used to trace stratospheric O_3 in the troposphere (Gaffney et al., 2005; Irlweck et al., 1997; Kritz et al., 1991; Zanis et al., 2003). Most of the tropospheric ^{7}Be is produced in the stratosphere and upper troposphere through the interactions of incoming cosmogenic particles with atmospheric components (such as nitrogen and oxygen), adsorbed onto the aerosols, and washed out through precipitation. Because of its short half-life and well-defined source term, the naturally occurring radionuclide ^{7}Be in the troposphere can be a sensitive indicator for quantifying the influence of STT (Gaffney et al., 2005; Kaste et al., 2002). Based on the correlations between the concentrations of O_3 and ^{7}Be in the urban air of Houston and Phoenix, for instance, Gaffney et al. (2005) evaluated the transport of O_3 from the lower stratosphere/upper troposphere to the surface. In addition, to the STT, however, both the long-range lateral transport and in situ photochemical reactions (such as the photolysis of NO_2) are also important for controlling the concentration of tropospheric O_3. Therefore, the correlations between O_3 and ^{7}Be activity concentrations are often unclear (Gaffney et al., 2005). Past results imply that the information based only on the concentrations of O_3 and ^{7}Be is insufficient for characterizing the origin of tropospheric O_3, especially for those supplied through STT.

The stable isotopic compositions of atmospheric trace gases have been widely used to identify the origin and/or reaction paths of these gases (Kendall et al., 2007; Nakagawa et al., 2005; Shingubara et al., 2021; Thiemens and Heidenreich, 1983; Tsunogai et al., 1999, 2003, 2020). In addition to the traditional isotopes, a unique and distinctive triple oxygen isotopic composition (Δ^{17}O; the definition will be presented in Sect 1.2) has been used as a powerful tracer of the origin and/or behavior of the atmospheric components (Albertin et al., 2021; Hattori et al., 2021; Kawagucci et al., 2008; Nakagawa et al., 2018; Nelson et al., 2018; Thiemens, 1999; Tsunogai et al., 2010). In the case of tropospheric O_3, Δ^{17}O can be applied to trace stratospheric O_3 within the total tropospheric O_3 (Krankowsky et al., 2000, 2007; Lyons, 2001; Vicars and Savarino, 2014; Xu et al., 2021).

In this study, we determined the temporal variations in the Δ^{17}O of tropospheric O_3 in terminal positions ($\Delta^{17}O_{term}(O_3)$) at two stations in the eastern Asia region, Niigata and Nagoya in Japan, from 2018 to 2020 using a multistep nitrite-coated filter-pack method recently developed by Xu et al. (2021). Based on the relationship between the reciprocal of concentrations and $\Delta^{17}O_{term}$ of tropospheric O_3, we determined the Δ^{17}O of O_3 derived from the stratosphere, together with that produced at the surface altitude. Moreover, we quantified the mixing ratios of stratospheric O_3 within tropospheric O_3 (O_3 produced in the stratosphere and transported into the troposphere through STT) during the observation periods.

1.2 The triple oxygen isotopic composition of O_3

The stable isotopic compositions of O_3 are represented by the δ^{17}O and δ^{18}O values. The delta (δ) values were calculated as $R_{sample} / R_{standard} - 1$, where R is the ^{17}O/^{16}O ratio for δ^{17}O (or ^{18}O/^{16}O ratio for δ^{18}O) in the sample (R_{sample}) and standard reference material (Vienna Standard Mean Ocean Water, VSMOW) ($R_{standard}$). In this study, we used the Δ^{17}O signature defined by the following equation, which is frequently used for Δ^{17}O of NO_3^- (Böhlke et al., 2003; Coplen et al., 2004; Kaiser et al., 2007; Miller, 2002; Nelson et al., 2018; Tsunogai et al., 2010, 2011, 2014, 2016):

$$\Delta^{17}O = \frac{1+\delta^{17}O}{(1+\delta^{18}O)^{\beta}} - 1, \quad (1)$$

where the constant β is 0.5279 (Kaiser et al., 2007; Nakagawa et al., 2018; Nelson et al., 2018; Tsunogai et al., 2016, 2018).

The values of Δ^{17}O defined by the power law (Equation (1)) are different from those defined by the linear definition ($\Delta^{17}O = \delta^{17}O - 0.52 \times \delta^{18}O$) adopted in some of the previous O_3 studies (Ishino et al., 2017; Savarino et al., 2016; Vicars et al., 2012; Vicars and Savarino, 2014). Our Δ^{17}O of O_3 would have been (1.4 ± 0.1) ‰ higher if we had used this linear definition for calculation (see

https://doi.org/10.5194/acp-2021-1099
Preprint. Discussion started: 26 April 2022

Atmospheric Chemistry and Physics Discussions

Table S1 in the Supporting Information). Compared with the linear definition, $\Delta^{17}O$ based on the power-law definition is more stable during "mass-dependent" isotope fractionation processes (Kaiser et al., 2007). Thus, we used the $\Delta^{17}O$ defined by Equation (1) because it is always stable regardless of the progress of any partial removal reaction, such as that between O_3 and NO_2^- (reaction R1). Then, we can obtain the accurate $\Delta^{17}O$ of O_3 from those of NO_3^- based on the power-law definition. However, variations in $\Delta^{17}O$ based on the power-law definition are nonlinear distributions during mixing fractions with different $\Delta^{17}O$ values. In the calculation performed in this study (Sect 3), however, the deviations in $\Delta^{17}O$ of O_3 were less than 0.2 ‰. Because these deviations are smaller than the standard error associated with the determination of $\Delta^{17}O$ of O_3, we disregarded this effect in our discussion. Unless otherwise noted, the number after the mean represents the standard error of the mean (SE).

2 Experimental

2.1 Multistep nitrite-coated filter-pack system

The tropospheric O_3 collections were performed by passing air through a multistep nitrite-coated filter-pack system described in detail by Xu et al. (2021). The principle of O_3 collection underlying this method is filter-based chemical trapping, in which O_3 reacts with nitrite (NO_2^-) in the aqueous phase to form NO_3^- (Liu et al., 2001; Michalski and Bhattacharya, 2009; Vicars et al., 2012):

$$NO_2^- + O_3 \rightarrow NO_3^- + O_2. \quad \text{(R1)}$$

Because only O atoms in the terminal positions of O_3 react with NO_2^- (Liu et al., 2001; Michalski and Bhattacharya, 2009), the $\Delta^{17}O_{term}(O_3)$ can be estimated from NO_3^- produced on nitrite-coated filters via reaction R1 (Xu et al., 2021). In this study, we assumed that the reaction of nitrite with O_3 to nitrate follows a mass-dependent fractionation relationship (power-law with slope of 0.5279).

The NO_2^- solution used to coat the glass fiber filters was prepared following the method described by Xu et al. (2021). Based on the method of O_3 collection outlined by Xu et al. (2021), the first and second stages of the filter-pack system are 0.45 μm nylon filters, and the third, fourth, and fifth stages are the nitrite-coated filters that collect O_3 via reaction R1.

2.2 Sampling sites

In this study, samples of tropospheric O_3 in ambient air outside our laboratory building at Nagoya University in the city of Nagoya (Fig. S1; 35°9′7″ N, 136°58′19″ E; 67 m a.s.l.), located on the Pacific coast of central Japan, were collected from 25 January 2019 to 24 June 2020 (n = 36). Samples collected from September 2017 to May 2018 (n = 18) at the same location were reported by Xu et al. (2021). In this study, the tropospheric O_3 in the ambient air was collected at a flow rate of 5.0 L min^{-1} (293 K and 1 bar) for one week during the day (06:00–18:00 local time) and at night (18:00–06:00 local time), respectively, to capture possible diurnal variations in $\Delta^{17}O$ of O_3. The O_3 concentration data monitored continuously by the Atmospheric Environmental Regional Observation System (Ministry of the Environment Government of Japan) at nearby (< 2 km) Takigawa Elementary School station (AEROS, 2018, 2019, 2020) was used for the O_3 concentrations at our station at Nagoya University. The data of atmospheric radionuclide concentrations determined by the Nuclear Regulation Authority of Japan for every two-month period (NRA, 2018, 2019, 2020) were used to estimate the average ^7Be activity concentrations during sampling.

Tropospheric O_3 samples were also collected at the Niigata-Maki National Acid Deposition Monitoring Station (Fig. S1; 37°45'32″ N, 138°53'3″ E), located on a coastal plain on the Sea of Japan coast from 19 March 2018 to 21 October 2019 (n = 20). The samples were collected using a multistep nitrite-coated filter-pack system at a flow rate of 5.0 L min^{-1} (293 K and 1 bar) for one week. The mixing ratio of O_3 was measured continuously using a standard UV absorption monitor (model APOA-360, HORIBA Co., Ltd.,

https://doi.org/10.5194/acp-2021-1099
Preprint. Discussion started: 26 April 2022

Atmospheric Chemistry and Physics Discussions

Japan). The data of ^{7}Be determined by the Nuclear Regulation Authority of Japan for every two-month period (NRA, 2018, 2019, 2020) was also used to estimate the average concentrations during sampling.

After each collection period, the NO_3^- accumulated on the nitrite-coated filters was extracted using 400 mL (the Nagoya samples) or 500 mL (the Niigata samples) of Milli-Q water, passed through a 0.2 μm filter, and stored at 4 °C until the concentrations and isotopic compositions of NO_3^- were measured.

2.3 Analysis

The concentrations of NO_3^- and NO_2^- were measured simultaneously by ion chromatography (Prominence HIC-SP, Shimadzu, Japan) within a few days after sampling. The error (standard error of the mean) at the determined concentration was ± 3 % (Tsunogai et al., 2016). To determine the stable isotopic compositions of NO_3^-, each sample solution was chemically converted to N_2O using an azide-acetic acid buffer and spongy cadmium (Xu et al., 2021).

The stable isotopic compositions ($\delta^{18}O$ and $\Delta^{17}O$) of N_2O converted from NO_3^- in each vial were determined using a continuous-flow IRMS (CF-IRMS) system. The analytical procedures used for this system were the same as those detailed in previous studies (Hirota et al., 2010; Komatsu et al., 2008). We repeated the analyses for each solution sample three times to attain high precision for $\delta^{18}O$ and $\Delta^{17}O$. The standard error of the mean was better than ±0.5 ‰ for $\delta^{18}O$ and ±0.2 ‰ for $\Delta^{17}O$. The obtained values of $\Delta^{17}O$ for N_2O derived from NO_3^- in each sample were compared with those derived from our local laboratory nitrate standards (Nakagawa et al., 2013; Tsunogai et al., 2014, 2018) calibrated against the international standards of USGS34 and USGS35 (Böhlke et al., 2003; Kaiser et al., 2007). Because of the isotope fractionation that occurred during the thermal decomposition of N_2O (Komatsu et al., 2008), the $\delta^{18}O$ values for the measurement of O_2 converted from N_2O in O_3 samples were corrected using the relationship between the measured $\delta^{18}O$ of O_2 (N_2O thermal decomposition) and N_2O in other NO_3^- samples, where $\delta^{18}O$ of N_2O was calibrated against our local laboratory nitrate standards in the following days. All $\delta^{18}O$ and $\Delta^{17}O$ values of NO_3^- were normalized to the VSMOW scale.

2.4 Calculation of $\Delta^{17}O$ and $\delta^{18}O$ of tropospheric O_3

We obtained the oxygen isotopic compositions of NO_3^- produced via reaction R1 ($\Delta^{17}O(NO_3^-)$), from which the changes in $\Delta^{17}O$ caused by the contribution of nitrate blank were corrected. The $\Delta^{17}O(NO_3^-)$ in the filter-pack system was obtained from the intercept of the linear relationship between the reciprocal of the measured amounts of NO_3^- (n) and $\Delta^{17}O$ of NO_3^- ($\Delta^{17}O_n(NO_3^-)$) on each nitrite-coated filter (Keeling, 1958; Xu et al., 2021). This process followed the weighted least squares approach developed by York et al. (2004), in which the differences in the magnitude of errors among individual data were considered using an Excel sheet provided by Cantrell (2008).

From the value of $\Delta^{17}O(NO_3^-)$ estimated for each sampling, the $\Delta^{17}O$ of O_3 in terminal positions ($\Delta^{17}O_{term}(O_3)$) can thus be estimated by using a simple mass balance (Vicars et al., 2012; Vicars and Savarino, 2014):

$$\Delta^{17}O_{term}(O_3) = 3 \times \Delta^{17}O(NO_3^-) - 2 \times \Delta^{17}O(NO_2^-), \quad (2)$$

where $\Delta^{17}O(NO_2^-)$ denotes the $\Delta^{17}O$ of NO_2^- on the filters ((0.02 ± 0.03) ‰; Xu et al., 2021).

In addition to the $\Delta^{17}O_{term}(O_3)$, we can relate the amount of the nitrate blank (n_b) with $\Delta^{17}O_n(NO_3^-)$ and $\Delta^{17}O(NO_3^-)$ using the equations shown below (Xu et al., 2021):

$$n_b = n \times (\Delta^{17}O(NO_3^-) - \Delta^{17}O_n(NO_3^-) / (\Delta^{17}O(NO_3^-) - \Delta^{17}O_b(NO_3^-)), \quad (3)$$

where $\Delta^{17}O_b(NO_3^-)$ denotes the $\Delta^{17}O$ of the nitrate blank on the nitrite-coated filters ((−0.14 ± 0.1) ‰; Xu et al., 2021). In this study, we estimated n_b for each nitrite-coated filter from both n and $\Delta^{17}O_n(NO_3^-)$ on the nitrite-coated filters. The mean value of n_b ($\overline{n_b}$) was estimated and considered as the amount of the nitrate blank for each sample.

https://doi.org/10.5194/acp-2021-1099
Preprint. Discussion started: 26 April 2022

Atmospheric Chemistry and Physics Discussions

To estimate the $\delta^{18}O$ of tropospheric O_3 in terminal positions before the collection on the nitrite-coated filters ($\delta^{18}O_{term}(O_3)$), we used the measured amount and $\delta^{18}O$ of NO_3^- on the nitrite-coated filters. We estimated the amount of tropospheric O_3 at initial (N_0) and then calculated the $\delta^{18}O_{term}(O_3)$ using the equations of Rayleigh and mass balance on the nitrite-coated filters to correct the isotope fractionation during the reaction R1, which has been described in detail by Xu et al. (2021).

By using the quantity of NO_3^- measured on filter i of the nitrite-coated filters (n_i) and $\bar{n}_b$, we can estimate *the* N_0 value as follows (Xu et al., 2021):

$$n\_i = n_i - \bar{n}_b, \quad (4)$$

$$\ln n\_i = -k \times i + \ln [N_0 \times (e^k - 1)], \quad (5)$$

where n_i denotes the quantity of O_3-derived O atoms that react with NO_2^- at filter i of the nitrite-coated filters through reaction R1, and k is the first-order rate constant for each ambient O_3 collection. By fitting a regression line to the relationships between i (along the x-axis) and $\ln n\_i$ (on the y-axis) of the nitrite-coated filters sampled simultaneously, we can estimate the values of N_0 from the intercept of the regression line.

Therefore, the $\delta^{18}O_{term}(O_3)$ can be estimated from the following equation below (Xu et al., 2021):

$$\delta^{18}O_{term}(O_3) = [(n\_1 + 2n\_2 - N_0) \times n\_1 \times \delta^{18}O_{n\_1} + (N_0 - n\_1) \times n\_2 \times \delta^{18}O_{n\_2}] / [N_0 \times (n\_2 - n\_1) + n\_1 \times (n\_1 + n\_2)], \quad (6)$$

where n_1 and n_2 denote the amounts of O_3-derived O atoms that reacted with the NO_2^- at filter first and second stages of the nitrite-coated filters through reaction R1, respectively; and $\delta^{18}O_{n\_1}$ and $\delta^{18}O_{n\_2}$ denote the O_3-derived O atoms that reacted with NO_2^- through reaction R1 were converted to NO_3^- on the filter first and second stages, respectively. The uncertainties of the $\delta^{18}O_{term}(O_3)$ during the calculations were estimated using the error propagation formulas.

3 Results

The temporal variations in O_3 concentrations, $\Delta^{17}O_{term}(O_3)$, and $\delta^{18}O_{term}(O_3)$ observed in Nagoya and Niigata are shown in Figs. 1 and 2, respectively, together with those reported by Xu et al. (2021). At Nagoya, $\Delta^{17}O_{term}(O_3)$ varied from (35.2 ± 0.5) ‰ to (42.1 ± 0.9) ‰ with a mean value and standard deviation (1σ) of (37.5 ± 1.5) ‰ (Fig. 1b), and $\delta^{18}O_{term}(O_3)$ varied from (96.9 ± 3.1) ‰ to (168.9 ± 4.5) ‰ with a mean value and standard deviation (1σ) of (139.3 ± 21.1) ‰ (Fig. 1c). Additionally, the $\Delta^{17}O_{term}(O_3)$ showed diurnal variations with an average $\Delta^{17}O_{term}$ difference of (1.4 ± 0.7) ‰ (1σ) between daytime (higher) and nighttime (lower). The mean $\Delta^{17}O_{term}(O_3)$ and their standard deviations (1σ) were (38.2 ± 1.5) ‰ and (36.8 ± 1.2) ‰ in the daytime and nighttime, respectively, and the mean $\delta^{18}O_{term}(O_3)$ and their standard deviations (1σ) were (139.8 ± 20.8) ‰ and (138.9 ± 20.8) ‰ in the daytime and nighttime, respectively.

https://doi.org/10.5194/acp-2021-1099
Preprint. Discussion started: 26 April 2022

Atmospheric Chemistry and Physics Discussions

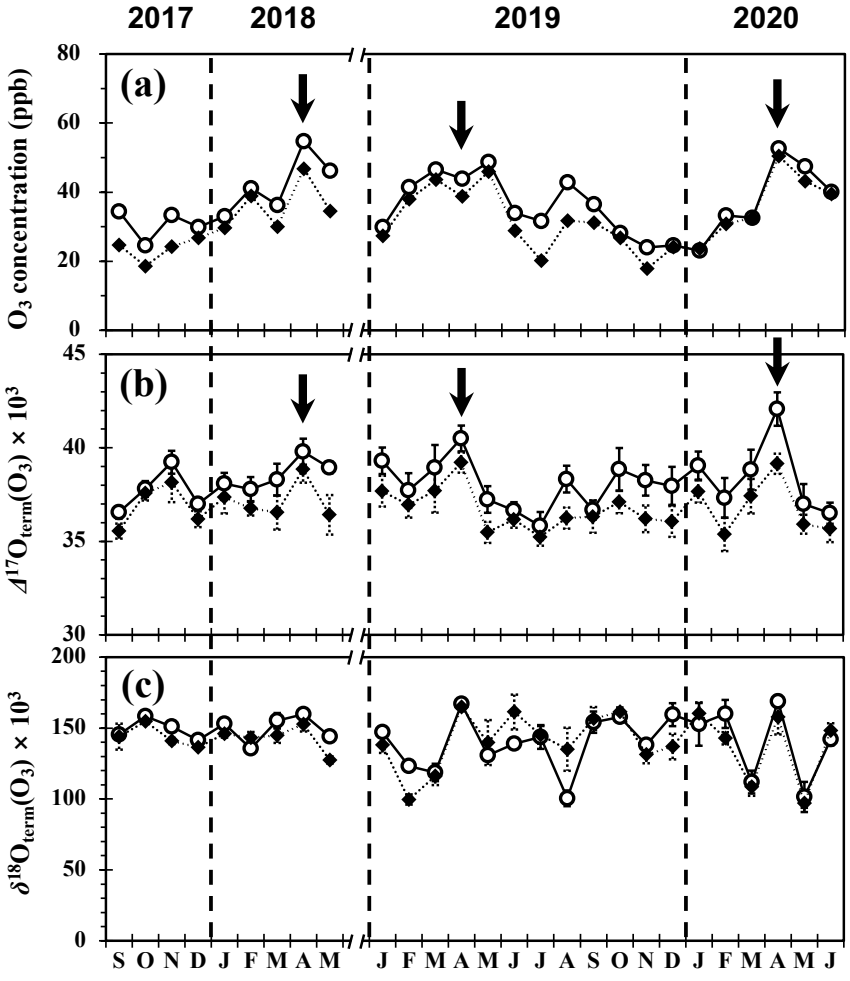

Figure 1. Temporal variations in concentrations, $\Delta^{17}O_{term}(O_3)$, and $\delta^{18}O_{term}(O_3)$ at Nagoya (a, b, and c), respectively. Open circles and close diamonds represent the daytime and nighttime, respectively. Vertical error bars represent the uncertainty of the least-squares method. The data sets from September 2017 to May 2018 were already reported in Xu et al. (2021).

At Niigata, $\Delta^{17}O_{term}(O_3)$ varied from (34.2 ± 0.8) ‰ to (41.4 ± 1.4) ‰ with a mean value and standard deviation (1σ) of (37.0 ± 1.7) ‰ (Fig. 2b), and $\delta^{18}O_{term}(O_3)$ varied from (99.4 ± 4.3) ‰ to (166.7 ± 1.2) ‰ with a mean value and standard deviation (1σ) of (140.6 ± 19.4) ‰ (Fig. 2c).

https://doi.org/10.5194/acp-2021-1099
Preprint. Discussion started: 26 April 2022

Atmospheric Chemistry and Physics Discussions

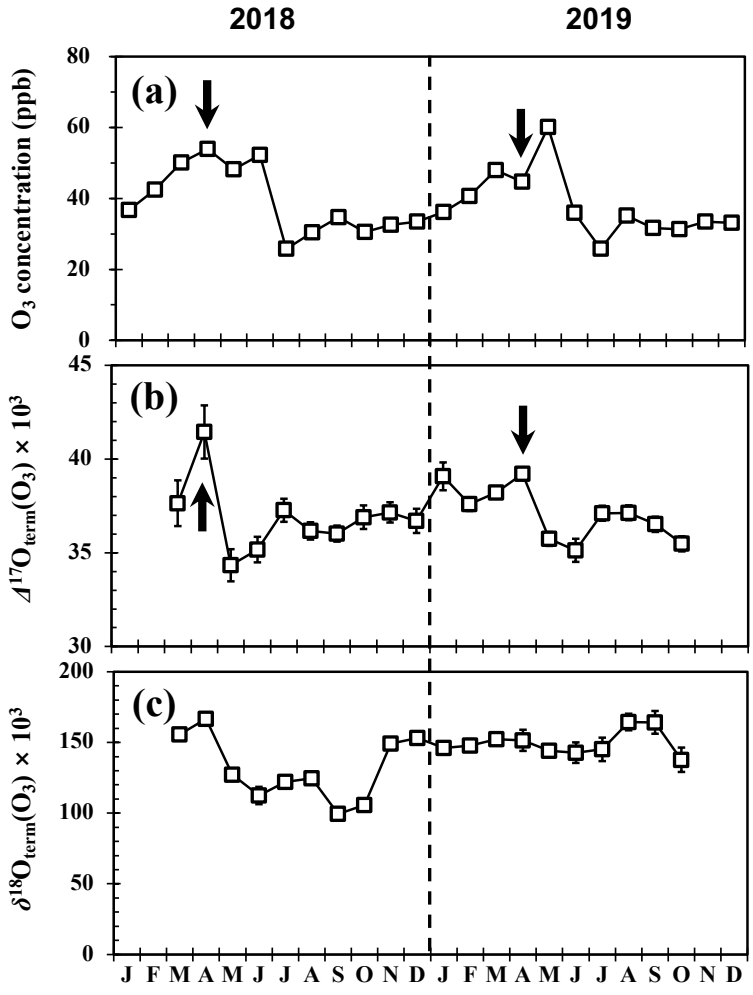

Figure 2. Temporal variations in concentrations, $\Delta^{17}O_{term}(O_3)$, and $\delta^{18}O_{term}(O_3)$ at Niigata (a, b, and c), respectively. Vertical error bars represent the uncertainty of the least-squares method.

The mean $\Delta^{17}O_{term}(O_3)$ of the tropospheric O_3 determined in this study ((37.5 ± 1.5) ‰ (1σ) at Nagoya and (37.0 ± 1.7) ‰ (1σ) at Niigata) is comparable with those reported in previous studies determined using the cryogenic trapping technique ((34.2 ± 4.3) ‰ (1σ) and (38.0 ± 6.6) ‰ (1σ) ; Johnston and Thiemens, 1997; Krankowsky et al., 1995) and the single nitrite-coated filter method ((37.3 ± 2.0) ‰ (1σ) and (37.7 ± 1.6) ‰ (1σ); Vicars and Savarino, 2014), all of which were recalculated from the original to the same $\Delta^{17}O$ definition adopted in this study.

The mean $\delta^{18}O_{term}(O_3)$ at Nagoya ((139.3 ± 21.1) ‰, (1σ)) and Niigata ((140.6 ± 19.4) ‰, (1σ)) coincided with those determined at Nagoya ((146.3 ± 8.5) ‰, (1σ)) in our previous study using the same method (Xu et al., 2021).

The data of atmospheric ^7Be in Nagoya and Niigata, determined by the Nuclear Regulation Authority of Japan, are summarized in Table S2 (NRA, 2018, 2019, 2020). Because all ^7Be data was obtained every two months, we calculated the weighted-average $\Delta^{17}O_{term}(O_3)$ using both concentrations and $\Delta^{17}O_{term}$ of tropospheric O_3 in the two months to discuss the relationship between ^7Be data and the $\Delta^{17}O_{term}(O_3)$ (Table S2).

https://doi.org/10.5194/acp-2021-1099
Preprint. Discussion started: 26 April 2022

Atmospheric Chemistry and Physics Discussions

4 Discussion

4.1 Diurnal variation

The variations in the $\Delta^{17}O_{term}(O_3)$ between the daytime and nighttime during 2019 and 2020 in Nagoya (1.4 ‰ on average) exceeded the uncertainty of the $\Delta^{17}O_{term}(O_3)$ measurements (±0.8 ‰ on average), implying that the diurnal variations were significant. Xu et al. (2021) assumed that $\Delta^{17}O_{term}(O_3)$ was higher in the free troposphere than in the surface boundary layer and proposed that the formation of a stable boundary layer during nighttime, which hindered vertical convection in the troposphere, was responsible for the diurnal $\Delta^{17}O_{term}(O_3)$ variations. Based on the photochemical data and model of DeMore et al. (1994) and Wayne (1991), Lyons (2001) predicted an increase in the bulk $\Delta^{17}O$ of O_3 produced in situ in the troposphere from 35 ‰ to 40 ‰ in proportion to the altitudes from 0 to 10 km, which corresponds to the $\Delta^{17}O_{term}(O_3)$ from 52.5 ‰ to 60 ‰. Although $\Delta^{17}O_{term}(O_3)$ reported by Lyons (2001) deviated from those determined in this study, the increasing trend in $\Delta^{17}O$ of O_3 in accordance with the altitudes of production supported our interpretation of the diurnal variation of $\Delta^{17}O_{term}(O_3)$.

4.2 Seasonal variation

Our previous study also found a clear $\Delta^{17}O$ maximum in April 2018 during the observation period from September 2017 to May 2018 at Nagoya (Xu et al., 2021), while all past measurements of $\Delta^{17}O_{term}(O_3)$ at mid-latitudes reported small seasonal variations. In this study, we further verified the maximum in April every year, showing (40.5 ± 0.7) ‰ in 2019 and (42.1 ± 0.9) ‰ in 2020 at Nagoya, and (41.4 ± 1.4) ‰ in 2018 and (39.2 ± 0.3) ‰ in 2019 at Niigata (shown by arrows in Figs. 1 and 2), all of which exceeded the ranges of the standard deviation (1σ) of the mean $\Delta^{17}O$: $\Delta^{17}O_{term}(O_3)$ of (37.5 ± 1.4) ‰ at Nagoya, and (37.0 ± 1.6) ‰ at Niigata, respectively. Because the total uncertainties of $\Delta^{17}O_{term}(O_3)$ analysis were approximately 2.6 ‰ in previous studies (Vicars et al., 2012; Vicars and Savarino, 2014), it might be difficult to detect seasonal variation, considering the maximum was in April in past studies.

Not only $\Delta^{17}O_{term}(O_3)$ but also O_3 concentrations were at a higher level throughout the year in April (shown by arrows in Figs. 1 and 2). Because both the concentrations and $\Delta^{17}O$ of stratospheric O_3 are higher than those of tropospheric O_3 (Krankowsky et al., 2007; Lyons, 2001; Vicars and Savarino, 2014), the enhancement of STT from late winter to early spring (Austin and Follows, 1991; Beekmann et al., 1994; Muramatsu et al., 2008) was highly responsible for the maximum $\Delta^{17}O_{term}(O_3)$ in April. We would like to verify this possibility using ^{7}Be as a tracer of STT.

4.3 Correlation between ^{7}Be activity concentrations and $\Delta^{17}O_{term}(O_3)$

The radionuclide ^{7}Be has been used to trace stratospheric O_3 supplied through STT (Gaffney et al., 2005; Lee et al., 2007). Because the ^{7}Be data usually shows a maximum during winter and spring in the troposphere of Japan every year due to STT (Akata et al., 2018; Narazaki and Fujitaka, 2009), STT is highly responsible for the high $\Delta^{17}O$ we found for tropospheric O_3 in April. To verify that stratospheric O_3 was responsible for the high $\Delta^{17}O_{term}(O_3)$, we plotted the $\Delta^{17}O_{term}(O_3)$ as a function of ^{7}Be activity concentrations for each observation period and place (Fig. 3). The significant correlation between ^{7}Be data and $\Delta^{17}O_{term}(O_3)$ shown in Fig. 3 ($R^2 = 0.53$; $p < 0.01$) implies that the STT is highly responsible for the elevated $\Delta^{17}O_{term}(O_3)$ in the troposphere, and that the $\Delta^{17}O_{term}(O_3)$ can be explained by a simple mixing between stratospheric O_3 and tropospheric O_3. If we extrapolated the linear correlation to stratospheric ^{7}Be activity concentration known to range from 160 mBq m^{-3} to 580 mBq m^{-3} (Kaste et al., 2002), the stratospheric $\Delta^{17}O_{term}(O_3)$ increased from 117.5 ‰ to 332.3 ‰. Although the $\Delta^{17}O_{term}(O_3)$ showed a significant linear correlation

https://doi.org/10.5194/acp-2021-1099
Preprint. Discussion started: 26 April 2022

Atmospheric Chemistry and Physics Discussions

with ^{7}Be at activity concentrations less than 5 mBq m^{-3}, it is difficult to assume the same linear correlation until high ^{7}Be activity concentrations up to 580 mBq m^{-3} are reached, because both ^{7}Be and O_3 are heterogeneous in the stratosphere. While ^{7}Be data shows the maximum concentration at altitudes lower than 20 km in the stratosphere (Delaygue et al., 2015; Koch and Rind, 1998), for instance, O_3 shows a maximum concentration of approximately 25 km at mid-latitudes in the Northern Hemisphere (Dütsch, 1978; Zou and Gao, 1997). Furthermore, stratospheric O_3 shows significant seasonal variation as well (Stolarski et al., 2014). Therefore, we estimated the $\Delta^{17}O$ of stratospheric O_3 using the relationship between O_3 concentrations and $\Delta^{17}O$ of O_3 in the troposphere, as explained in the next section.

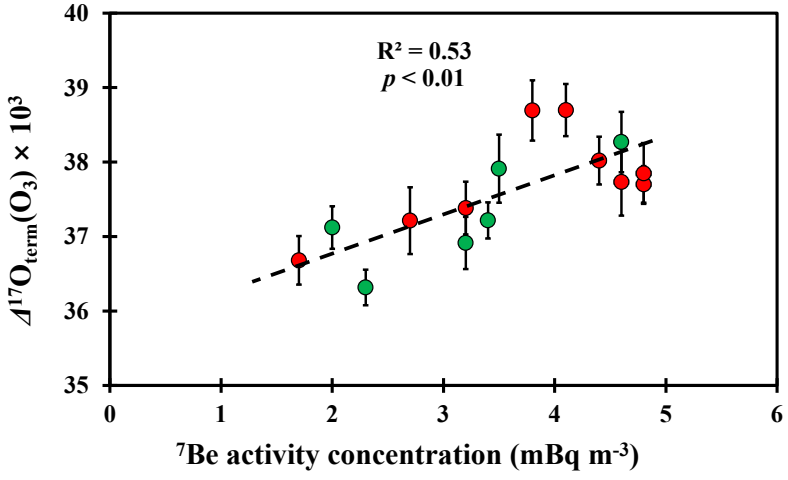

Figure 3. Red and green circles represent the relationship between atmospheric ^{7}Be activity concentrations and $\Delta^{17}O_{term}(O_3)$ in each two-month period both at Nagoya and Niigata, respectively. The dotted line is the least-squares fitting to these circles. The error bars represent the analytical precision (SE).

4.4 Estimating $\Delta^{17}O_{term}(O_3)$ of O_3 derived from stratosphere

One of the remarkable features of the relationship between the reciprocal of tropospheric O_3 concentrations (1/[O_3]) and $\Delta^{17}O_{term}(O_3)$ (Fig. 4) was that the dispersion in the $\Delta^{17}O_{term}$ became larger in accordance with the O_3 enrichment (i.e., 1/[O_3] depletion), while the $\Delta^{17}O_{term}$ was almost uniform in the O_3-deleted region (i.e., high 1/[O_3] region). The low-level O_3 (i.e., O_3 in the high 1/[O_3] region) with concentrations less than 20 parts per billion (ppb) (v/v) level and $\Delta^{17}O_{term}$ around 37 ‰ should represent background O_3 in the troposphere (orange circles in Fig. 4).

https://doi.org/10.5194/acp-2021-1099
Preprint. Discussion started: 26 April 2022

Atmospheric Chemistry and Physics Discussions

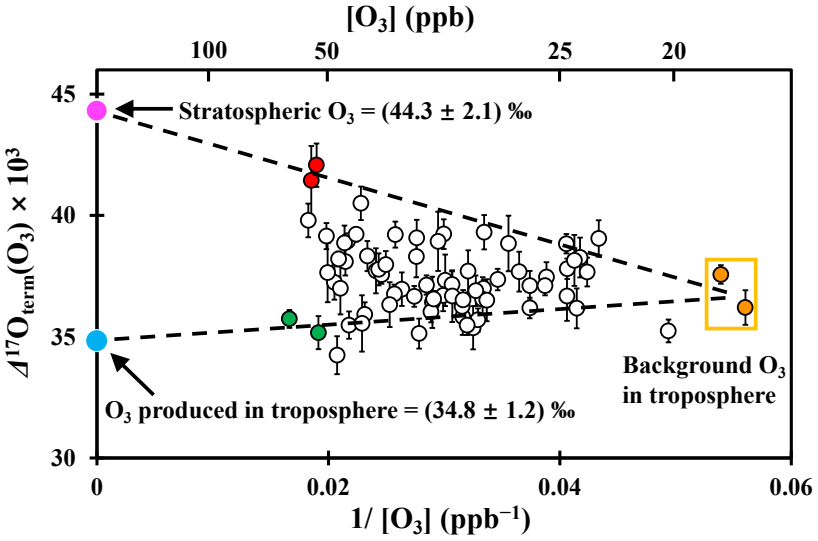

285 **Figure 4.** Relationship between the reciprocal of tropospheric O_3 concentrations and $\Delta^{17}O_{term}(O_3)$ in Nagoya and Niigata. The pink, orange, and blue circles represent the different sources to $\Delta^{17}O_{term}(O_3)$ determined in this study. The red represent high O_3 concentration (> 50 ppb) and $\Delta^{17}O_{term}(O_3)$ (> 40 ‰). The green circles represent high O_3 concentration (> 50 ppb) but low $\Delta^{17}O_{term}(O_3)$ (< 37 ‰). The error bars represent the analytical precision (SE).

290 The concentration of O_3 in the troposphere is controlled by both physical and chemical processes. The representative processes are: (i) photochemical production in the stratosphere and supplied through STT (Archibald et al., 2020); (ii) in situ production of O_3 in the troposphere from precursors such as NO_x (Logan, 1985; Wild, 2007); (iii) in situ removal of O_3 in the troposphere through photochemical reactions, such as NO + O_3; and (iv) removal of O_3 in the troposphere through deposition onto the surface of plants, soils, water, snow, and ice (Archibald et al., 2020; Gaffney et al., 2005). On the other hand, we assumed that $\Delta^{17}O$ was almost
295 stable during the latter partial removal processes of O_3 (Nos. iii and iv), because oxygen isotopic fractionations associated with the chemical reaction processes follow the relation $\Delta\delta^{17}O + 1 = (\Delta\delta^{18}O + 1)^{\beta}$, where $\beta \cong 0.5279$ (Chakraborty and Chakraborty, 2003). Thus, the variations in $\Delta^{17}O$ of tropospheric O_3 reflect the changes in the mixing ratios of O_3 supplied through STT (No. i) and O_3 produced in situ in the troposphere through photochemical reactions (No. ii). Considering that the difference in the altitude of production, troposphere or stratosphere was the major factor controlling $\Delta^{17}O$ of O_3 (Krankowsky et al., 2007; Lyons, 2001; Vicars
300 and Savarino, 2014), variations in their mixing ratios were highly responsible for the observed increase in the dispersion of the $\Delta^{17}O$ values of tropospheric O_3 in accordance with the increase in tropospheric O_3 concentration. In other words, the samples showing both the highest concentrations (> 50 ppb) and the highest level of $\Delta^{17}O_{term}(O_3)$ (> 40 ‰) obtained at Nagoya and Niigata in April (red circles in Fig. 4) were supplied through the simple mixing of stratospheric O_3 with background O_3 in the troposphere. On the other hand, the samples with the highest concentrations (> 50 ppb) but the lowest level of $\Delta^{17}O_{term}(O_3)$ (< 37 ‰) obtained
305 at Niigata in June 2018 and May 2019 (green circles in Fig. 4) were supplied through the simple mixing of O_3 produced in situ in the troposphere through photochemical reactions with background O_3. The continuous measurements and model simulations of tropospheric O_3 also supported that both O_3 produced in situ in domestic air and O_3 produced in polluted urban air in the East Asian region and transported through lateral transports were responsible for the enhancement of O_3 during late spring and early summer (May to June) in Japan (Pochanart et al., 2015; Tanimoto, 2009; Tanimoto et al., 2005). Based on this interpretation, the observed
310 $\Delta^{17}O_{term}(O_3)$ in Nagoya and Niigata can be explained by mixing of the three components: background O_3 in the troposphere,

https://doi.org/10.5194/acp-2021-1099
Preprint. Discussion started: 26 April 2022

Atmospheric Chemistry and Physics Discussions

stratospheric O_3 supplied to the troposphere via STT ($\Delta^{17}O_{STT}$), and O_3 produced in situ in the troposphere through photochemical reactions ($\Delta^{17}O_{sur}$) (Fig. 4).

As shown in Fig. 4, we estimated $\Delta^{17}O_{STT}$ to be (44.3 ± 2.1) ‰ by extrapolating the linear mixing line between background O_3 (orange circles in Fig. 4) and the high O_3 with high $\Delta^{17}O$ samples enriched in stratospheric O_3 (red circles in Fig. 4); and $\Delta^{17}O_{sur}$ to be (34.8 ± 1.2) ‰ by extrapolating the linear mixing line between background O_3 and the high O_3 with low $\Delta^{17}O$ samples enriched in O_3 produced in situ in the troposphere (green circles in Fig. 4). The standard error of the mean in $\Delta^{17}O_{STT}$ and $\Delta^{17}O_{sur}$ was obtained according to the propagation law of error using the equation provided by Sambuichi et al. (2021). The estimated $\Delta^{17}O_{STT}$ agreed well with those measured in a previous study of stratospheric O_3 at altitudes ranging from 20 km to more than 30 km using the cryogenic trapping technique ((48.2 ± 6.2) ‰; Krankowsky et al., 2007).

4.5 Stratosphere–troposphere transport of O_3

Using the $\Delta^{17}O_{STT}$ and $\Delta^{17}O_{sur}$ values estimated in the previous section, we can estimate the concentrations of O_3 that were produced in the stratosphere but supplied through STT ($C_{STT}(O_3)$, ppb) for all tropospheric air using a simple isotope mass balance:

$$C_{STT}(O_3) = C_{total}(O_3) \times f_{STT} \quad (7)$$

$$f_{STT} = (\Delta^{17}O - \Delta^{17}O_{sur} \times f_{sur}) / \Delta^{17}O_{STT}, \quad (8)$$

$$f_{STT} = 1 - f_{sur}, \quad (9)$$

where $C_{total}(O_3)$ denotes the O_3 concentrations in ambient air (ppb); $\Delta^{17}O$ denotes the $\Delta^{17}O_{term}(O_3)$ measured in Nagoya and Niigata, and f_{STT} and f_{sur} denote the fractions of O_3 supplied through STT and through photochemical reactions at surface altitude, respectively, in each O_3. By using the $\Delta^{17}O_{sur}$ ((34.8 ± 1.2) ‰) and $\Delta^{17}O_{STT}$ ((44.3 ± 2.1) ‰) estimated in this study, we estimated the $C_{STT}(O_3)$ in Nagoya and Niigata over the years from 2017 to 2020, including those studied by Xu et al. (2021).

As shown in Figs. 5 and 6, $C_{STT}(O_3)$ varied from (0.9 ± 2.8) ppb to (40.3 ± 12.4) ppb with the mean values and standard deviations (1σ) of (13.4 ± 8.0) ppb and (7.2 ± 5.5) ppb in the daytime and nighttime at Nagoya, respectively, and from (–3.0 ± 7.5) ppb to (37.7 ± 14.5) ppb with a mean value and standard deviation (1σ) of (9.1 ± 9.0) ppb at Niigata.

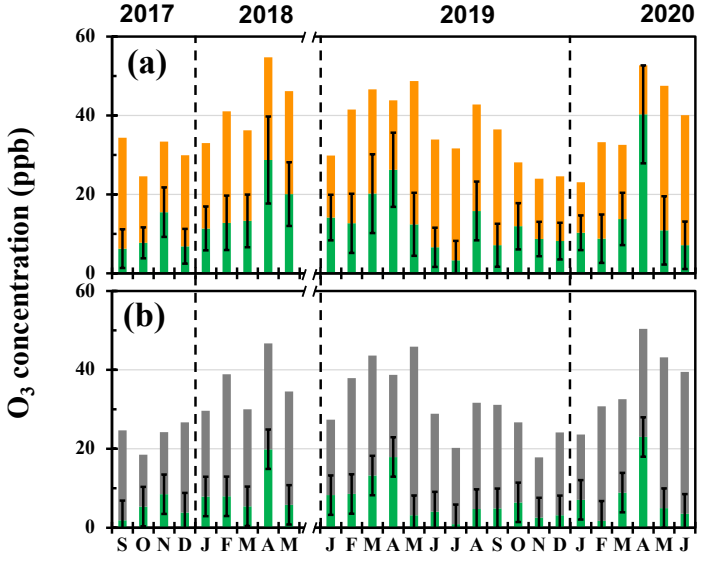

Figure 5. The concentrations of O_3 supplied by stratosphere–troposphere transport ($C_{STT}(O_3)$) estimated in daytime (a) and nighttime (b) at Nagoya, respectively. The green bars are the $C_{STT}(O_3)$ values. The orange and grey bars represent $C_{total}(O_3)$ during

https://doi.org/10.5194/acp-2021-1099
Preprint. Discussion started: 26 April 2022

Atmospheric Chemistry and Physics Discussions

daytime and nighttime, respectively. Vertical error bars represent the standard error of $C_{STT}(O_3)$ values using the error propagation formulas.

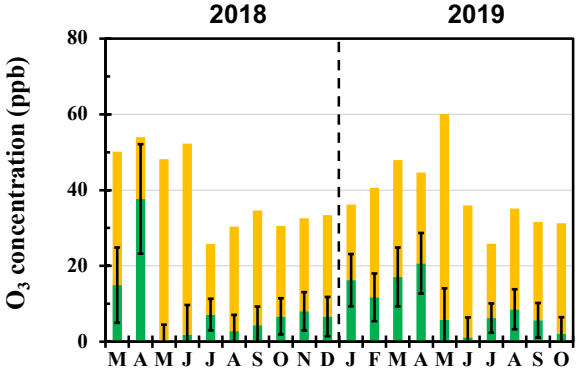

Figure 6. The concentrations of O_3 supplied by stratosphere–troposphere transport ($C_{STT}(O_3)$) estimated in Niigata. The green bars are the $C_{STT}(O_3)$ values. The yellow bars represent $C_{total}(O_3)$. Vertical error bars represent the standard error of $C_{STT}(O_3)$ values using the error propagation formulas.

The common feature in the two sites was that $C_{STT}(O_3)$ was the highest in spring (March to May), with a mean value of (15.9 ± 2.1) ppb and lowest in summer (June to August) with a mean value of (5.3 ± 1.0) ppb. This implies that the synoptic-scale meteorological changes from spring to summer were responsible for the changes in $C_{STT}(O_3)$. The high $C_{STT}(O_3)$ in spring appears to occur in conjunction with the spring O_3 maximum (Monks, 2000). Previous studies have suggested that the STT (Austin and Midgley, 1994; Itahashi et al., 2020; Oltmans et al., 2004) and/or the enhanced O_3 levels in polluted air masses transported from East Asia (Itahashi et al., 2009; Tanimoto, 2009; Tanimoto et al., 2005) are responsible for the O_3 maximum in spring. In our study, the $C_{STT}(O_3)$ values were high in March and April, but low in May at both sites (Figs. 5 and 6), suggesting that the STT was mainly responsible for the enhancement of tropospheric O_3 concentrations in early spring; however, photochemical production in the troposphere was responsible for the enhancement in late spring. The intrusion of stratospheric air associated with the jet stream and the Asian monsoon was responsible for the differences. That is, stratospheric O_3 is transported into the troposphere through the mechanism of tropopause folding or cut-off lows in early spring (Austin and Midgley, 1994; Carmichael et al., 1998; Danielsen, 1968). On the other hand, the long-range lateral transport of O_3 produced through anthropogenic emissions in the East Asian troposphere was responsible for the high O_3 concentrations in late spring (Itahashi et al., 2009; Tanimoto, 2009; Tanimoto et al., 2005).

The f_{STT} data in Nagoya and Niigata, estimated using Equations (8) and (9), are summarized in Table 1. It is worth noting that the seasonality of f_{STT} with a minimum in the summer and increasing from autumn to spring, was observed at both sites (Table 1), agreed well with the seasonal variations in f_{STT} determined for the East Japan region obtained by Nagashima et al. (2010) based on CHASER modeling calculations, while the mean f_{STT} in spring ((35.3 ± 9.5) %, 2SE) and summer ((15.6 ± 6.1) %, 2SE) during the years from 2017 to 2020 were somewhat higher than those estimated from 2000 to 2005 in the previous study (21.1 % in spring and 5.9 % in summer, Nagashima et al., 2010).

https://doi.org/10.5194/acp-2021-1099
Preprint. Discussion started: 26 April 2022

Atmospheric Chemistry and Physics Discussions

Table 1. Seasonal mean contributions of stratosphere–troposphere transport (f_{STT}) during the sampling periods.

Location	season	collection period [a]	f_{STT} (%)
Nagoya	Spring	D	45.4 ± 7.1
		N	28.0 ± 6.0
	Summer	D	22.1 ± 7.2
		N	11.0 ± 2.8
	Autumn	D	31.6 ± 4.8
		N	20.8 ± 4.2
	Winter	D	33.2 ± 2.8
		N	20.3 ± 3.2
	Mean	D	36.3 ± 4.2
		N	22.3 ± 3.3
Niigata	Spring	all-day	30.6 ± 11.1
	Summer		13.5 ± 3.7
	Autumn		16.7 ± 3.1
	Winter		31.3 ± 7.6
	Mean		23.4 ± 5.1

[a] D and N denote the collection periods of daytime (06:00 to 18:00) and nighttime (18:00 to 6:00), respectively.

The difference in resolution between the observation and model is highly responsible for the observed discrepancy in f_{STT}. In addition, we ignored the O_3 produced in the upper troposphere originally and supplied to the surface through vertical convection in our calculation of f_{STT}, which could overestimate f_{STT}. Because global warming can increase the STT (Sudo et al., 2003), we should continue monitoring STT by measuring the $\Delta^{17}O$ of tropospheric O_3 to verify the temporal changes. Further improvement in the calculation of f_{STT} for $\Delta^{17}O$ is required. Nevertheless, $\Delta^{17}O$ can be a novel tracer for evaluating the increase/decrease in f_{STT}.

5 Conclusion

The $\Delta^{17}O_{term}(O_3)$ of (37.5 ± 1.4) ‰ (1σ) and (37.0 ± 1.7) ‰ (1σ) observed in the tropospheric air at Nagoya and Niigata, respectively, agreed with previous studies. Based on the significant correlation between ^7Be activity concentrations and $\Delta^{17}O_{term}(O_3)$, we concluded that the STT was responsible for the elevated $\Delta^{17}O_{term}$ of tropospheric O_3, especially in April. In addition, we found that both concentrations and the $\Delta^{17}O_{term}$ of tropospheric O_3 can be explained by mixing between the three components: background O_3 in the troposphere, stratospheric O_3 supplied to the troposphere through STT, and O_3 produced in situ in the troposphere through photochemical reactions, and the estimated absolute concentrations of the stratospheric O_3 supplied through STT in the troposphere were highest in spring and lowest in summer. Moreover, the trend in seasonal variations of O_3 supplied through STT estimated in this study is in agreement with a previous study.

Data availability. The data used for the figures and the interpretations have been included in the Supplement.

Supplement. The supplement related to this article is available online.

https://doi.org/10.5194/acp-2021-1099
Preprint. Discussion started: 26 April 2022

Atmospheric Chemistry and Physics Discussions

Author contributions. UT, FN, KS, and HT designed the study. HX and KS collected samples. HX, UT, and FN performed data analysis. HX and UT prepared the manuscript with contributions from all co-authors. All authors have given approval to the final version of the manuscript.

Competing interests. The authors declare that they have no conflict of interest.

Acknowledgements. We are grateful to Masanori Ito, Ryo Shingubara, Takashi Sanbuichi, and other present and past members of the Biogeochemistry Group, Nagoya University, for their valuable support throughout this study. This work was supported by a grant-in-aid for scientific research from the Ministry of Education, Culture, Sports, Science and Technology of Japan (MEXT, Japan) under grant numbers 26241006, 17H00780, 19K22908, and 19H04254, and by a grant from Steel Foundation for Environmental Protection Technology.

References

AEROS: Data report 2018, Network center for Atmospheric Environmental Regional Observation System, Nagoya. https://soramame.env.go.jp/, cited 2018.

AEROS: Data report 2019, Network center for Atmospheric Environmental Regional Observation System, Nagoya. https://soramame.env.go.jp/, cited 2019.

AEROS: Data report 2020, Network center for Atmospheric Environmental Regional Observation System, Nagoya. https://soramame.env.go.jp/, cited 2020.

Akata, N., Shiroma, Y., Ikemoto, N., Kato, A., Hegeds, M., Tanaka, M., Kakiuchi, H. and Kovács, T.: Atmospheric Concentration and Deposition Flux of Cosmogenic Beryllium-7 at Toki, Central Part of Japan, Radiat. Environ. Med., 7(1), 47–52, 2018.

Akimoto, H.: Global Air Quality and Pollution, Science (80-.)., 302(5651), 1716–1719, doi:10.1126/science.1092666, 2003.

Albertin, S., Savarino, J., Bekki, S., Barbero, A. and Caillon, N.: Measurement report: Nitrogen isotopes ($\delta^{15}N$) and first quantification of oxygen isotope anomalies ($\Delta^{17}O$, $\delta^{18}O$) in atmospheric nitrogen dioxide, Atmos. Chem. Phys., 21(13), 10477–10497, doi:10.5194/acp-21-10477-2021, 2021.

Archibald, A. T., Neu, J. L., Elshorbany, Y. F., Cooper, O. R., Young, P. J., Akiyoshi, H., Cox, R. A., Coyle, M., Derwent, R. G., Deushi, M., Finco, A., Frost, G. J., Galbally, I. E., Gerosa, G., Granier, C., Griffiths, P. T., Hossaini, R., Hu, L., Jöckel, P., Josse, B., Lin, M. Y., Mertens, M., Morgenstern, O., Naja, M., Naik, V., Oltmans, S., Plummer, D. A., Revell, L. E., Saiz-Lopez, A., Saxena, P., Shin, Y. M., Shahid, I., Shallcross, D., Tilmes, S., Trickl, T., Wallington, T. J., Wang, T., Worden, H. M. and Zeng, G.: Tropospheric ozone assessment report: A critical review of changes in the tropospheric ozone burden and budget from 1850 to 2100, Elem. Sci. Anthr., 8(1), 1–53, doi:10.1525/elementa.2020.034, 2020.

Austin, J. F. and Follows, M. J.: The ozone record at Payerne: An assessment of the cross-tropopause flux, Atmos. Environ., 25(9), 1873–1880, doi:10.1016/0960-1686(91)90270-H, 1991.

Austin, J. F. and Midgley, R. P.: The climatology of the jet stream and stratospheric intrusions of ozone over Japan, Atmos. Environ., 28(1), 39–52, doi:10.1016/1352-2310(94)90021-3, 1994.

Avnery, S., Mauzerall, D. L., Liu, J. and Horowitz, L. W.: Global crop yield reductions due to surface ozone exposure: 1. Year 2000 crop production losses and economic damage, Atmos. Environ., 45(13), 2284–2296, doi:10.1016/j.atmosenv.2010.11.045, 2011.

https://doi.org/10.5194/acp-2021-1099
Preprint. Discussion started: 26 April 2022

Atmospheric Chemistry and Physics Discussions

Beekmann, M., Ancellet, G. and Megie, G.: Climatology of tropospheric ozone in southern Europe and its relation to potential vorticity, J. Geophys. Res., 99(D6), 12841–12853, doi:10.1029/94jd00228, 1994.

Böhlke, J. K., Mroczkowski, S. J. and Coplen, T. B.: Oxygen isotopes in nitrate: New reference materials for $^{18}O:^{17}O:^{16}O$ measurements and observations on nitrate-water equilibration, Rapid Commun. Mass Spectrom., 17(16), 1835–1846, doi:10.1002/rcm.1123, 2003.

Cantrell, C. A.: Technical Note: Review of methods for linear least-squares fitting of data and application to atmospheric chemistry problems, Atmos. Chem. Phys., 8(17), 5477–5487, doi:10.5194/acp-8-5477-2008, 2008.

Carmichael, G. R., Uno, I., Phadnis, M. J., Zhang, Y. and Sunwoo, Y.: Tropospheric ozone production and transport in the springtime in east Asia, J. Geophys. Res. Atmos., 103(3339), 10649–10671, doi:10.1029/97jd03740, 1998.

Chakraborty, S. and Chakraborty, S.: Isotopic fractionation of the O_3-nitric oxide reaction, Curr. Sci., 85(8), 1210–1212, 2003.

Coplen, T. B., Böhlke, J. K. and Casciotti, K. L.: Using dual-bacterial denitrification to improve $\delta^{15}N$ determinations of nitrates containing mass-independent ^{17}O, Rapid Commun. Mass Spectrom., 18(3), 245–250, doi:10.1002/rcm.1318, 2004.

Danielsen, E. F.: Stratospheric-Tropospheric Exchange Based on Radioactivity, Ozone and Potential Vorticity, J. Atmos. Sci., 25(3), 502–518, 1968.

Delaygue, G., Bekki, S. and Bard, E.: Modelling the stratospheric budget of beryllium isotopes, Tellus B Chem. Phys. Meteorol., 67(1), doi:10.3402/tellusb.v67.28582, 2015.

DeMore, W. B., Sander, S. P., Golden, D. M., Hampson, R. F., Kurylo, M. J., Howard, C. J., Ravishankara, A. R., Kolb, C. E. and Molina, M. J.: Chemical kinetics and photochemical data for use in stratospheric modeling., 1983.

Dütsch, H. U.: Vertical ozone distribution on a global scale, Pure Appl. Geophys. PAGEOPH, 116, 511–529, doi:10.1007/BF01636904, 1978.

Finlayson-Pitts, B. J. and Pitts, J. N.: Tropospheric air pollution: ozone, airborne toxics, polycyclic aromatic hydrocarbons, and particles, Science (80-.)., 276(5315), 1045–1052, doi:10.1126/science.276.5315.1045, 1997.

Gaffney, J. S., Marley, N. A., Cunningham, M. M. and Kotamarthi, V. R.: Beryllium-7 measurements in the houston and phoenix urban areas: An estimation of upper atmospheric ozone contributions, J. Air Waste Manag. Assoc., 55(8), 1228–1235, doi:10.1080/10473289.2005.10464707, 2005.

Hansen, J. E. and Sato, M.: Trends of measured climate forcing agents, Proc. Natl. Acad. Sci. U. S. A., 98(26), 14778–14783, doi:10.1073/pnas.261553698, 2001.

Hattori, S., Iizuka, Y., Alexander, B., Ishino, S., Fujita, K., Zhai, S., Sherwen, T., Oshima, N., Uemura, R., Yamada, A., Suzuki, N., Matoba, S., Tsuruta, A., Savarino, J. and Yoshida, N.: Isotopic evidence for acidity-driven enhancement of sulfate formation after SO_2 emission control, Sci. Adv., 7(19), doi:10.1126/sciadv.abd4610, 2021.

Hirota, A., Tsunogai, U., Komatsu, D. D. and Nakagawa, F.: Simultaneous determination of $\delta^{15}N$ and $\delta^{18}O$ of N_2O and $\delta^{13}C$ of CH_4 in nanomolar quantities from a single water sample, Rapid Commun. Mass Spectrom., 24, 1457–1466, doi:10.1002/rcm, 2010.

Irlweck, K., Hinterdorfer, K. and Karg, V.: Beryllium-7 and ozone correlations in surface atmosphere, Naturwissenschaften, 84(8), 353–356, doi:10.1007/s001140050409, 1997.

Ishino, S., Hattori, S., Savarino, J., Jourdain, B., Preunkert, S., Legrand, M., Caillon, N., Barbero, A., Kuribayashi, K. and Yoshida, N.: Seasonal variations of triple oxygen isotopic compositions of atmospheric sulfate, nitrate, and ozone at Dumont d'Urville, coastal Antarctica, Atmos. Chem. Phys., 17(5), 3713–3727, doi:10.5194/acp-17-3713-2017, 2017.

Itahashi, S., Yumimoto, K., Uno, I., Ohara, T., Kurokawa, J., Shimizu, A., Yamamoto, S., Oishi, O. and Iwamoto, S.: Analysis of transboundary air pollution occurred during Spring 2007 over East Asia using CMAQ [in Japanese with English abstract], J.

https://doi.org/10.5194/acp-2021-1099
Preprint. Discussion started: 26 April 2022

Japan Soc. Atmos. Environ., 44(4), 175–185, 2009.

Itahashi, S., Mathur, R., Hogrefe, C., L. Napelenok, S. and Zhang, Y.: Modeling stratospheric intrusion and trans-Pacific transport on tropospheric ozone using hemispheric CMAQ during April 2010 – Part 1: Model evaluation and air mass characterization for stratosphere–troposphere transport, Atmos. Chem. Phys., 20(6), 3397–3413, doi:10.5194/acp-20-3397-2020, 2020.

Jerrett, M., Burnett, R. T., Pope, C. A., Ito, K., Thurston, G., Krewski, D., Shi, Y., Calle, E. and Thun, M.: Long-Term Ozone Exposure and Mortality, N. Engl. J. Med., 360(11), 1085–1095, doi:10.1056/nejmoa0803894, 2009.

Johnston, J. C. and Thiemens, M. H.: The isotopic composition of tropospheric ozone in three environments, J. Geophys. Res. Atmos., 102(21), 25395–25404, doi:10.1029/97jd02075, 1997.

Kaiser, J., Hastings, M. G., Houlton, B. Z., Röckmann, T. and Sigman, D. M.: Triple oxygen isotope analysis of nitrate using the denitrifier method and thermal decomposition of N_2O, Anal. Chem., 79(2), 599–607, doi:10.1021/ac061022s, 2007.

Kaste, J. M., Norton, S. A. and Hess, C. T.: Environmental chemistry of Beryllium-7, Rev. Mineral. Geochemistry, 271–290, doi:10.2138/rmg.2002.50.6, 2002.

Kawagucci, S., Tsunogai, U., Kudo, S., Nakagawa, F., Honda, H., Aoki, S., Nakazawa, T., Tsutsumi, M. and Gamo, T.: Long-term observation of mass-independent oxygen isotope anomaly in stratospheric CO_2, Atmos. Chem. Phys., 8(20), 6189–6197, doi:10.5194/acp-8-6189-2008, 2008.

Keeling, D.: The concentration and isotopic abundances of atmospheric carbon dioxide in rural areas, Geochim. Cosmochim. Acta, 13, 322–334, 1958.

Kendall, C., Elliott, E. M. and Wankel, S. D.: Tracing Anthropogenic Inputs of Nitrogen to Ecosystems, Stable Isot. Ecol. Environ. Sci. Second Ed., 375–449, doi:10.1002/9780470691854.ch12, 2007.

Koch, D. and Rind, D.: Beryllium 10/beryllium 7 as a tracer of stratospheric transport, J. Geophys. Res. Atmos., 103(D4), 3907–3917, doi:10.1029/97JD03117, 1998.

Komatsu, D. D., Ishimura, T., Nakagawa, F. and Tsunogai, U.: Determination of the $^{15}N/^{14}N$, $^{17}O/^{16}O$, and $^{18}O/^{16}O$ ratios of nitrous oxide by using continuous-flow isotope-ratio mass spectrometry, Rapid Commun. Mass Spectrom., 24, 1457–1466, doi:10.1002/rcm, 2008.

Krankowsky, D., Bartecki, F., Klees, G. G., Mauersberger, K., Schellenbach, K. and Stehr, J.: Measurement of heavy isotope enrichment in tropospheric ozone, Geophys. Res. Lett., 22(13), 1713–1716, doi:10.1029/95GL01436, 1995.

Krankowsky, D., Lammerzahl, P. and Mauersberger, K.: Isotopic measurements of stratospheric ozone, Geophys. Res. Lett., 27(17), 2593–2595, doi:10.1029/2000GL011812, 2000.

Krankowsky, D., Lämmerzahl, P., Mauersberger, K., Janssen, C., Tuzson, B. and Röckmann, T.: Stratospheric ozone isotope fractionations derived from collected samples, J. Geophys. Res. Atmos., 112(8), 1–7, doi:10.1029/2006JD007855, 2007.

Kritz, M. A., Rosner, S. W., Danielsen, E. F. and Selkirk, H. B.: Air mass origins and troposphere-to-stratosphere exchange associated with mid-latitude cyclogenesis and tropopause folding inferred from ^{7}Be measurements, J. Geophys. Res., 96(D9), 17405–17414, doi:10.1029/91jd01358, 1991.

Lee, H. N., Tositti, L., Zheng, X. and Bonasoni, P.: Analyses and comparisons of variations of ^{7}Be, ^{210}Pb, and $^{7}Be/^{210}Pb$ with ozone observations at two Global Atmosphere Watch stations from high mountains, J. Geophys. Res. Atmos., 112(5), 1–11, doi:10.1029/2006JD007421, 2007.

Liu, Q., Schurter, L. M., Muller, C. E., Aloisio, S., Francisco, J. S. and Margerum, D. W.: Kinetics and mechanisms of aqueous ozone reactions with bromide, sulfite, hydrogen sulfite, iodide, and nitrite ions, Inorg. Chem., 40(17), 4436–4442, doi:10.1021/ic000919j, 2001.

Logan, J. A.: Tropospheric ozone: seasonal behavior, trends, and anthropogenic influence, J. Geophys. Res., 90(D6), 10463–10482,

doi:10.1029/JD090iD06p10463, 1985.

Lyons, J. R.: Transfer of mass-independent fractionation in ozone to other oxygen-containing radicals in the atmosphere, Geophys. Res. Lett., 28(17), 3231–3234, doi:10.1029/2000GL012791, 2001.

Michalski, G. and Bhattacharya, S. K.: The role of symmetry in the mass independent isotope effect in ozone, Proc. Natl. Acad. Sci. U. S. A., 106(14), 5493–5496, doi:10.1073/pnas.0812755106, 2009.

Miller, M. F.: Isotopic fractionation and the quantification of ^{17}O anomalies in the oxygen three-isotope system: an appraisal and geochemical significance, Geochim. Cosmochim. Acta, 66(11), 1881–1889, 2002.

Monks, P. S.: A review of the observations and origins of the spring ozone maximum, Atmos. Environ., 34(21), 3545–3561, doi:10.1016/S1352-2310(00)00129-1, 2000.

Muramatsu, H., Yoshizawa, S., Abe, T., Ishii, T., Wada, M., Horiuchi, Y. and Kanekatsu, R.: Variation of ^{7}Be concentration in surface air at Nagano, Japan, J. Radioanal. Nucl. Chem., 275(2), 299–307, doi:10.1007/s10967-007-7056-8, 2008.

Nagashima, T., Ohara, T., Sudo, K. and Akimoto, H.: The relative importance of various source regions on East Asian surface ozone, Atmos. Chem. Phys., 10(22), 11305–11322, doi:10.5194/acp-10-11305-2010, 2010.

Nakagawa, F., Tsunogai, U., Komatsu, D. D., Yamada, K., Yoshida, N., Moriizumi, J., Nagamine, K., Iida, T. and Ikebe, Y.: Automobile exhaust as a source of ^{13}C- and D-enriched atmospheric methane in urban areas, Org. Geochem., 36(5), 727–738, doi:10.1016/j.orggeochem.2005.01.003, 2005.

Nakagawa, F., Suzuki, A., Daita, S., Ohyama, T., Komatsu, D. D. and Tsunogai, U.: Tracing atmospheric nitrate in groundwater using triple oxygen isotopes: Evaluation based on bottled drinking water, Biogeosciences, 10(6), 3547–3558, doi:10.5194/bg-10-3547-2013, 2013.

Nakagawa, F., Tsunogai, U., Obata, Y., Ando, K., Yamashita, N., Saito, T., Uchiyama, S., Morohashi, M. and Sase, H.: Export flux of unprocessed atmospheric nitrate from temperate forested catchments: a possible new index for nitrogen saturation, Biogeosciences, 15(22), 7025–7042, doi:10.5194/bg-15-7025-2018, 2018.

Narazaki, Y. and Fujitaka, K.: Cosmogenic 7Be: Atmospheric Concentration and Deposition in Japan, Japanese J. Heal. Phys., 44(1), 95–105, doi:10.5453/jhps.44.95, 2009.

Nelson, D. M., Tsunogai, U., Ding, D., Ohyama, T., Komatsu, D. D., Nakagawa, F., Noguchi, I. and Yamaguchi, T.: Triple oxygen isotopes indicate urbanization affects sources of nitrate in wet and dry atmospheric deposition, Atmos. Chem. Phys., 18(9), 6381–6392, doi:10.5194/acp-18-6381-2018, 2018.

NRA: Data report 2018, Network center for Nuclear Regulation Authority of Japan, Nagoya and Niigata. https://www.kankyo-hoshano.go.jp/data/database/, cited 2018.

NRA: Data report 2019, Network center for Nuclear Regulation Authority of Japan, Nagoya and Niigata. https://www.kankyo-hoshano.go.jp/data/database/, cited 2019.

NRA: Data report 2020, Network center for Nuclear Regulation Authority of Japan, Nagoya and Niigata. https://www.kankyo-hoshano.go.jp/data/database/, cited 2020.

Oltmans, S. J., Johnson, B. J., Harris, J. M., Thompson, A. M., Liu, H. Y., Chan, C. Y., Vömel, H., Fujimoto, T., Brackett, V. G., Chang, W. L., Chen, J. P., Kim, J. H., Chan, L. Y. and Chang, H. W.: Tropospheric ozone over the North Pacific from ozonesonde observations, J. Geophys. Res. D Atmos., 109(15), doi:10.1029/2003JD003466, 2004.

Pochanart, P., Wang, Z. and Akimoto, H.: Boundary layer ozone transport from eastern China to Southern Japan: Pollution episodes observed during monsoon onset in 2004, Asian J. Atmos. Environ., 9(1), 48–56, doi:10.5572/ajae.2015.9.1.048, 2015.

Reich, P. B. and Amundson, R. G.: Ambient levels of ozone reduce net photosynthesis in tree and crop species, Science (80-.)., 230(4725), 566–570, doi:10.1126/science.230.4725.566, 1985.

https://doi.org/10.5194/acp-2021-1099
Preprint. Discussion started: 26 April 2022

Sambuichi, T., Tsunogai, U., Kura, K., Nakagawa, F. and Ohba, T.: High-precision $\Delta'^{17}O$ measurements of geothermal H_2O and MORB on the VSMOW–SLAP scale: evidence for active oxygen exchange between the lithosphere and hydrosphere, Geochem. J., 55, 25–33, doi:10.2343/geochemj.2.0644, 2021.

Savarino, J., Vicars, W. C., Legrand, M., Preunkert, S., Jourdain, B., Frey, M. M., Kukui, A., Caillon, N. and Roca, J. G.: Oxygen isotope mass balance of atmospheric nitrate at Dome C, East Antarctica, during the OPALE campaign, Atmos. Chem. Phys., 16(4), 2659–2673, doi:10.5194/acp-16-2659-2016, 2016.

Shingubara, R., Tsunogai, U., Ito, M., Nakagawa, F., Yoshikawa, S., Utsugi, M. and Yokoo, A.: Development of a drone-borne volcanic plume sampler, J. Volcanol. Geotherm. Res., 412, 107197, doi:10.1016/j.jvolgeores.2021.107197, 2021.

Silva, R. A., West, J. J., Zhang, Y., Anenberg, S. C., Lamarque, J. F., Shindell, D. T., Collins, W. J., Dalsoren, S., Faluvegi, G., Folberth, G., Horowitz, L. W., Nagashima, T., Naik, V., Rumbold, S., Skeie, R., Sudo, K., Takemura, T., Bergmann, D., Cameron-Smith, P., Cionni, I., Doherty, R. M., Eyring, V., Josse, B., Mackenzie, I. A., Plummer, D., Righi, M., Stevenson, D. S., Strode, S., Szopa, S. and Zeng, G.: Global premature mortality due to anthropogenic outdoor air pollution and the contribution of past climate change, Environ. Res. Lett., 8(3), doi:10.1088/1748-9326/8/3/034005, 2013.

Skärby, L., Ro-Poulsen, H., Wellburn, F. A. M. and Sheppard, L. J.: Impacts of ozone on forests: A European perspective, New Phytol., 139(1), 109–122, doi:10.1046/j.1469-8137.1998.00184.x, 1998.

Stohl, A., Wernli, H., James, P., Bourqui, M., Forster, C., Liniger, M. A., Seibert, P. and Sprenger, M.: A new perspective of stratosphere-troposphere exchange, Bull. Am. Meteorol. Soc., 84(11), 1565-1573+1473, doi:10.1175/BAMS-84-11-1565, 2003a.

Stohl, A., Bonasoni, P., Cristofanelli, P., Collins, W., Feichter, J., Frank, A., Forster, C., Gerasopoulos, E., Gäggeler, H., James, P., Kentarchos, T., Kromp-Kolb, H., Krüger, B., Land, C., Meloen, J., Papayannis, A., Priller, A., Seibert, P., Sprenger, M., Roelofs, G. J., Scheel, H. E., Schnabel, C., Siegmund, P., Tobler, L., Trickl, T., Wernli, H., Wirth, V., Zanis, P. and Zerefos, C.: Stratosphere-troposphere exchange: A review, and what we have learned from STACCATO, J. Geophys. Res. Atmos., 108(12), doi:10.1029/2002jd002490, 2003b.

Stolarski, R. S., Waugh, D. W., Wang, L., Oman, L. D., Douglass, A. R. and Newman, P. A.: Seasonal variation of ozone in the tropical lower stratosphere: Southern tropics are different from northern tropics, J. Geophys. Res. Atmos., 119(10), 6196–6206, doi:10.1038/175238c0, 2014.

Sudo, K., Takahashi, M. and Akimoto, H.: Future changes in stratosphere-troposphere exchange and their impacts on future tropospheric ozone simulations, Geophys. Res. Lett., 30(24), 2–5, doi:10.1029/2003GL018526, 2003.

Tanimoto, H.: Increase in springtime tropospheric ozone at a mountainous site in Japan for the period 1998-2006, Atmos. Environ., 43(6), 1358–1363, doi:10.1016/j.atmosenv.2008.12.006, 2009.

Tanimoto, H., Sawa, Y., Matsueda, H., Uno, I., Ohara, T., Yamaji, K., Kurokawa, J. I. and Yonemura, S.: Significant latitudinal gradient in the surface ozone spring maximum over East Asia, Geophys. Res. Lett., 32(21), 1–5, doi:10.1029/2005GL023514, 2005.

Thiemens, M. H.: Mass-independent isotope effects in planetary atmospheres and the early solar system, Science (80-.)., 283(5400), 341–345, doi:10.1126/science.283.5400.341, 1999.

Thiemens, M. H. and Heidenreich, J. E.: The mass-independent fractionation of oxygen: A novel isotope effect and its possible cosmochemical implications, Science (80-.)., 219(4588), 1073–1075, doi:10.1126/science.219.4588.1073, 1983.

Thompson, A. M.: The oxidizing capacity of the Earth's atmosphere: Probable past and future changes, Science (80-.)., 256(5060), 1157–1165, doi:10.1126/science.256.5060.1157, 1992.

Tsunogai, U., Yoshida, N. and Gamo, T.: Carbon isotopic compositions of C_2-C_5 hydrocarbons and methyl chloride in urban,

https://doi.org/10.5194/acp-2021-1099
Preprint. Discussion started: 26 April 2022

coastal, and maritime atmospheres over the western North Pacific, J. Geophys. Res., 104, 33–39, 1999.

Tsunogai, U., Hachisu, Y., Komatsu, D. D., Nakagawa, F., Gamo, T. and Akiyama, K. I.: An updated estimation of the stable carbon and oxygen isotopic compositions of automobile CO emissions, Atmos. Environ., 37(35), 4901–4910, doi:10.1016/j.atmosenv.2003.08.008, 2003.

Tsunogai, U., Komatsu, D. D., Daita, S., Kazemi, G. A., Nakagawa, F., Noguchi, I. and Zhang, J.: Tracing the fate of atmospheric nitrate deposited onto a forest ecosystem in Eastern Asia using $\Delta^{17}O$, Atmos. Chem. Phys., 10(4), 1809–1820, doi:10.5194/acp-10-1809-2010, 2010.

Tsunogai, U., Daita, S., Komatsu, D. D., Nakagawa, F. and Tanaka, A.: Quantifying nitrate dynamics in an oligotrophic lake using $\Delta^{17}O$, Biogeosciences, 8(3), 687–702, doi:10.5194/bg-8-687-2011, 2011.

Tsunogai, U., Komatsu, D. D., Ohyama, T., Suzuki, A., Nakagawa, F., Noguchi, I., Takagi, K., Nomura, M., Fukuzawa, K. and Shibata, H.: Quantifying the effects of clear-cutting and strip-cutting on nitrate dynamics in a forested watershed using triple oxygen isotopes as tracers, Biogeosciences, 11(19), 5411–5424, doi:10.5194/bg-11-5411-2014, 2014.

Tsunogai, U., Miyauchi, T., Ohyama, T., Komatsu, D. D., Nakagawa, F., Obata, Y., Sato, K. and Ohizumi, T.: Accurate and precise quantification of atmospheric nitrate in streams draining land of various uses by using triple oxygen isotopes as tracers, Biogeosciences, 13(11), 3441–3459, doi:10.5194/bg-13-3441-2016, 2016.

Tsunogai, U., Miyauchi, T., Ohyama, T., Komatsu, D. D., Ito, M. and Nakagawa, F.: Quantifying nitrate dynamics in a mesotrophic lake using triple oxygen isotopes as tracers, Limnol. Oceanogr., 63, S458–S476, doi:10.1002/lno.10775, 2018.

Tsunogai, U., Miyoshi, Y., Matsushita, T., Komatsu, D. D., Ito, M., Sukigara, C., Nakagawa, F. and Maruo, M.: Dual stable isotope characterization of excess methane in oxic waters of a mesotrophic lake, Limnol. Oceanogr., 65(12), 2937–2952, doi:10.1002/lno.11566, 2020.

UNEP and WMO: Integrated assessment of black carbon and tropospheric ozone: summary for decision makers, 2011.

Vicars, W. C. and Savarino, J.: Quantitative constraints on the ^{17}O-excess ($\Delta^{17}O$) signature of surface ozone: Ambient measurements from 50°N to 50°S using the nitrite-coated filter technique, Geochim. Cosmochim. Acta, 135, 270–287, doi:10.1016/j.gca.2014.03.023, 2014.

Vicars, W. C., Bhattacharya, S. K., Erbland, J. and Savarino, J.: Measurement of the ^{17}O-excess ($\Delta^{17}O$) of tropospheric ozone using a nitrite-coated filter, Rapid Commun. Mass Spectrom., 26(10), 1219–1231, doi:10.1002/rcm.6218, 2012.

Wayne, R. P., Chemistry of Atmospheres, second ed., Clarendon Press: Oxford, 1991.

Wild, O.: Modelling the global tropospheric ozone budget: Exploring the variability in current models, Atmos. Chem. Phys., 7(10), 2643–2660, doi:10.5194/acp-7-2643-2007, 2007.

Xu, H., Tsunogai, U., Nakagawa, F., Li, Y., Ito, M., Sato, K. and Tanimoto, H.: Determination of the triple oxygen isotopic composition of tropospheric ozone in terminal positions using a multistep nitrite-coated filter-pack system, Rapid Commun. Mass Spectrom., 35(15), 1–15, doi:10.1002/rcm.9124, 2021.

York, D., Evensen, N. M., Martínez, M. L. and De Basabe Delgado, J.: Unified equations for the slope, intercept, and standard errors of the best straight line, Am. J. Phys., 72(3), 367–375, doi:10.1119/1.1632486, 2004.

Zanis, P., Gerasopoulos, E., Priller, A., Schnabel, C., Stohl, A., Zerefos, C., Gäggeler, H. W., Tobler, L., Kubik, P. W., Kanter, H. J., Scheel, H. E., Luterbacher, J. and Berger, M.: An estimate of the impact of stratosphere-to-troposphere transport (STT) on the lower free tropospheric ozone over the Alps using ^{10}Be and ^{7}Be measurements, J. Geophys. Res. Atmos., 108(12), 1–9, doi:10.1029/2002jd002604, 2003.

Zhang, J. J., Wei, Y. and Fang, Z.: Ozone pollution: A major health hazard worldwide, Front. Immunol., 10(OCT), 1–10, doi:10.3389/fimmu.2019.02518, 2019.

https://doi.org/10.5194/acp-2021-1099
Preprint. Discussion started: 26 April 2022

Atmospheric Chemistry and Physics Discussions

Zou, H. and Gao, Y.: Vertical ozone profile over Tibet using SAGE I and II data, Adv. Atmos. Sci., 14(4), 505–512, doi:10.1007/s00376-997-0068-z, 1997.